

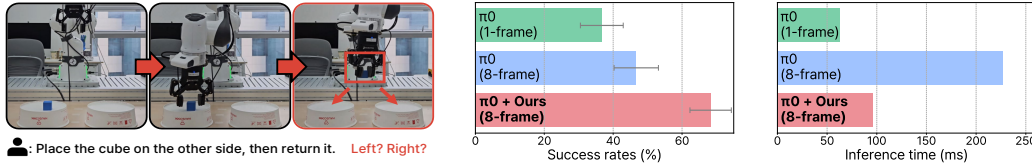
000 CONTEXTVLA: VISION-LANGUAGE-ACTION MODEL 001 WITH AMORTIZED MULTI-FRAME CONTEXT 002 003 004

005 **Anonymous authors**

006 Paper under double-blind review

007 008 ABSTRACT

009
010
011 Leveraging temporal context is crucial for success in partially observable robotic
012 tasks. However, prior work in behavior cloning has demonstrated inconsistent per-
013 formance gains when using multi-frame observations. In this paper, we introduce
014 ContextVLA, a policy model that robustly improves robotic task performance by
015 effectively leveraging multi-frame observations. Our approach is motivated by the
016 key observation that Vision-Language-Action models (VLA), *i.e.*, policy models
017 built upon a Vision-Language Model (VLM), more effectively utilize multi-frame
018 observations for action generation. This suggests that VLMs' inherent temporal
019 understanding capability enables them to extract more meaningful context from
020 multi-frame observations. However, the high dimensionality of video inputs in-
021 troduces significant computational overhead, making VLA training and inference
022 inefficient. To address this, ContextVLA compresses past observations into a sin-
023 gle context token, allowing the policy to efficiently leverage temporal context for
024 action generation. Our experiments show that ContextVLA consistently improves
025 over single-frame VLAs and achieves the benefits of full multi-frame training but
with reduced training and inference times.



026 (a) A task that requires temporal context

027 (b) Real-world task result

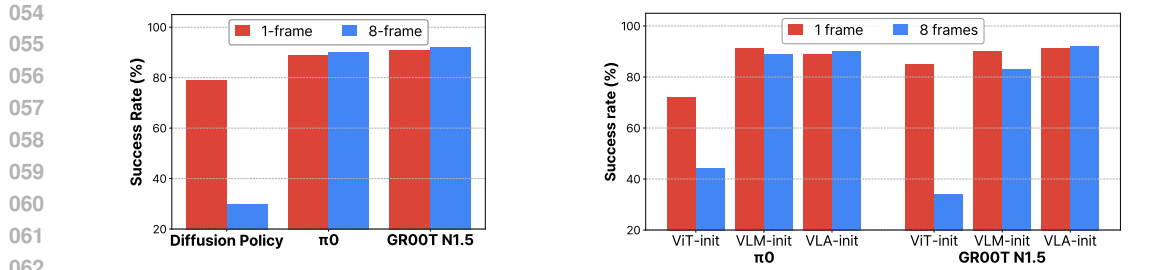
028 (c) Inference efficiency

029 Figure 1: **Overview.** (a) Many robotic tasks require temporal context to generate accurate actions.
030 (b) By leveraging multi-frame observations, our proposed method, ContextVLA, achieves higher
031 averaged success rates (%) over all baseline policies on real-world robotic tasks. (c) Moreover, our
032 framework gets benefits of multi-frame training with reduced inference latency.

033 1 INTRODUCTION

034 Many robotic tasks are inherently non-Markovian, *i.e.*, the optimal decision at a given timestep t
035 cannot be determined from the latest observation \mathbf{o}_t alone but requires past sequential observations
036 $\mathbf{o}_{1:t}$ (Kaelbling et al., 1998; Zheng et al., 2024; Shi et al., 2025). For instance, an object may become
037 occluded during manipulation (Shi et al., 2025). Solving long-horizon tasks may also require context
038 about the previous motions of a robot, and handling dynamic environments often involves tracking
039 the motion trajectories of moving objects (Zhang et al., 2025; Nasiriany et al., 2024). Consequently,
040 policy models must have capability to predict the actions based on the understanding of consecutive
041 input observations (*i.e.*, multi-frame observations) to perform real-world challenging task.

042 Despite its importance, recent behavior cloning (BC) policies usually have been trained with only a
043 single frame observation (Kim et al., 2024; Bjorck et al., 2025; Pertsch et al., 2025; GEAR, 2025).
044 This is mainly due to the mixed results reported in recent studies on training policy models with
045 multi-frame observations. Specifically, several works argue that multi-frame observations do im-
046 prove performance (Wu et al., 2023; Team et al., 2024; Cheang et al., 2024; Zheng et al., 2024;
047 Liu et al., 2025; Li et al., 2025), but surprisingly, many others have observed contradictory results;
048 namely, this training scheme can even lead to performance degradation (Muller et al., 2005; De Haan
049 et al., 2019; Wen et al., 2020; Spencer et al., 2021; Seo et al., 2023; Torne et al., 2025).



(a) Performance of recent policy models trained using either 1-frame or 8-frame observations.

(b) Performance of policy models of VLA architecture trained using either 1-frame or 8-frame observations under different weight initialization schemes.

Figure 2: **Effect of multi-frame observations for training various policy models.** We report the success rates (%) of various policy models fine-tuned on Square task from the Robomimic benchmark (Mandlekar et al., 2021). (a) When training policy models using multi-frame observations, traditional policy model (Diffusion policy) shows significant performance degradation, whereas recent Vision-Language-Action models (VLA; π_0 and GROOT N1.5) do not. (b) We find that the key factor in overcoming this problem is leveraging a pre-trained Vision-Language Model (VLM) to extract temporal information for action generation. ViT, VLM, and VLA-init indicate how the VLA architecture is initialized for training; we use a pre-trained vision encoder, VLM, or VLA, respectively, and other parameters are randomly initialized.

Contribution. We introduce a framework that enables BC policy models to effectively leverage multi-frame observations, thereby achieving consistent performance improvement across a wide range of manipulation tasks. To this end, we start by performing an analysis of why prior works have reported inconsistent gains from multi-frame observations. We find that while standard policies often suffer from performance degradation with multi-frame data, Vision-Language-Action models (VLA; Black et al. 2024; Bjorck et al. 2025), *i.e.*, policy models initialized from or conditioned on a Vision-Language Model (VLM; Beyer et al. 2024; Chen et al. 2025), mitigate this problem (Figure 2a). In particular, our analysis shows that the VLM serves as the key component in mitigating performance degradation (Figure 2b). This finding suggests that the VLM’s temporal understanding is key to extracting more meaningful context from videos for action generation. However, leveraging multi-frame observations for VLA training and inference significantly increases computational cost, as high-dimensional sequences must be processed by large VLMs (often >1 B parameters). Thus, it is important to develop efficient approaches for exploiting multi-frame information with VLAs.

Based on this analysis, we propose ContextVLA, an efficient framework that leverages a VLM’s temporal understanding to learn a BC policy model that utilizes multi-frame observations. Our key idea is to compress past observations into a single context token, which enables the VLA to efficiently capture temporal context (*e.g.*, the movement of a robot) to generate actions with reduced computation overhead. Specifically, ContextVLA first processes the full observation sequence using the initial blocks of the VLM backbone. It then aggregates the tokens from past observations into a single context token. Then the remaining VLM blocks process the sequence consisting of this new context token and the tokens for the current observation. After that, the resulting VLM features are fed into an action decoder to generate actions in either an autoregressive (Pertsch et al., 2025) or diffusion-based manner (Black et al., 2024; Bjorck et al., 2025).

We verify the effectiveness of our scheme through extensive experiments on various robotic manipulation benchmarks, including Libero (Liu et al., 2023a), Simpler-WidowX (Li et al., 2024b), and Robocasa (Nasiriany et al., 2024). Our results show that ContextVLA consistently improves the performance of recent state-of-the-art VLAs that use single-frame observations. For instance, on the Simpler-WidowX benchmark, ContextVLA improves the average success rate of π_0 (Black et al., 2024) by 14.4% (41.8% \rightarrow 56.2%). Moreover, we find that ContextVLA is particularly effective on long-horizon real-world robotic tasks that require temporal understanding (Figure 4b). For example, fine-tuning π_0 (Black et al., 2024) with our framework achieves a 65% success rate on the pick-and-place twice (PnP Twice) task, whereas the single-frame baseline gets only 25%. Finally, we show that ContextVLA enables efficient training and inference of multi-frame VLA models, delivering the benefits of multi-frame training while significantly reducing the training and inference costs.

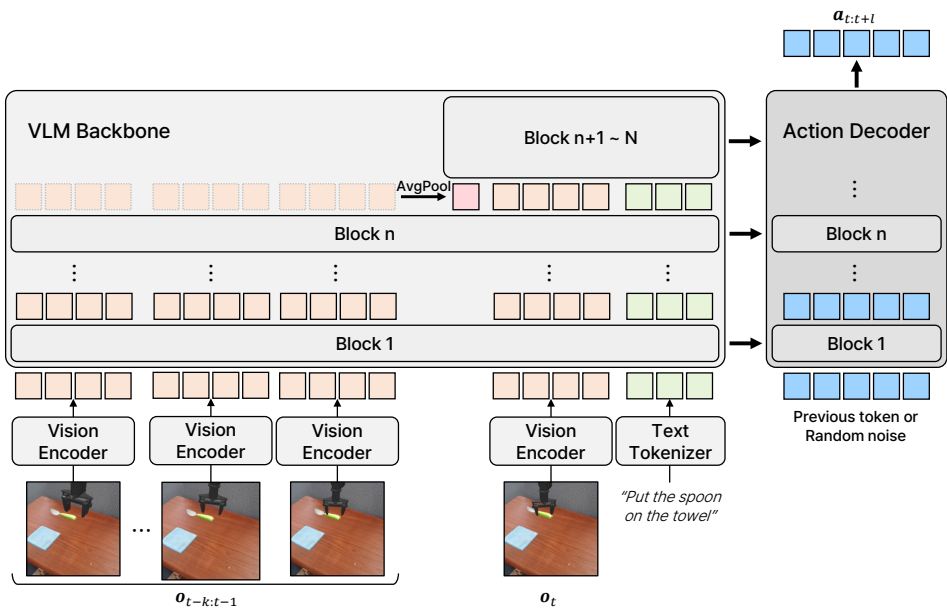


Figure 3: **Overview of ContextVLA.** We design an efficient Vision-Language-Action model (VLA) that generates actions using multi-frame visual observations. We use a Vision-Language Model (VLM) to encode observations $\mathbf{o}_{t-k:t}$, where we compress past observations $\mathbf{o}_{t-k:t-1}$ into a single context token \mathbf{m} at the VLM block n . We then leverage the VLM features to generate actions via either autoregressive modeling or diffusion-based modeling.

2 METHOD

In this section, we introduce ContextVLA, an efficient training framework for Vision-Language-Action models (VLA) that leverages *multi-frame* observations. In a nutshell, ContextVLA encodes hidden states of past visual observations into a compact global context token at the intermediate layer of Vision-Language-Model (VLM) backbone, while preserving the number of tokens of current observations. After that, these VLM features are fed into an action decoder to generate the action. We provide the overview of ContextVLA in Figure 3.

2.1 PRELIMINARIES

Problem Setup. Let $\tau = \{(\mathbf{o}_t, \mathbf{c}_t, \mathbf{a}_t)\}_{t=1}^T$ be an expert demonstration consisting of visual observation \mathbf{o}_t , language instruction \mathbf{c}_t , and robot action \mathbf{a}_t for each timestep t , and let $\mathcal{D} = \{\tau_i\}_{i=1}^N$ be a dataset consisting of expert demonstrations. Here, visual observation \mathbf{o}_t can be either single or multi-view depending on the environment. Moreover, we denote by $\mathbf{x}_{a:b}$ the sequence of consecutive vectors $[\mathbf{x}_a, \dots, \mathbf{x}_b]$ for $a < b$.

Given $\tau \in \mathcal{D}$, our goal is to train a policy model $\pi_\theta(\mathbf{a}_{t:t+l} | \mathbf{o}_{t-k:t}, \mathbf{c}_t)$, which predicts $l + 1$ future actions $\mathbf{a}_{t:t+l}$ of the robot (Zhao et al., 2023; Chi et al., 2023) from $k + 1$ -frame observations $\mathbf{o}_{t-k:t}$ and a language instruction \mathbf{c}_t . In particular, we aim this policy π_θ to leverage $k + 1$ -frame visual observations so that it understands not only the current state, but the context of past observations to generate actions. However, using longer past observations can dramatically increase computation and memory overheads by increasing input dimensionality that π_θ processes, resulting in inefficient training and inference. Therefore, we design π_θ to process past observations efficiently.

Multi-frame Vision-Language-Action Model. We design the policy π_θ as VLA, where it encodes visual observations $\mathbf{o}_{t-k:t}$ and a task instruction \mathbf{c}_t using a pre-trained VLM (Beyer et al., 2024; Bai et al., 2025; Chen et al., 2025), and uses the extracted features from the VLM to generate a robot action $\mathbf{a}_{t:t+l}$. Action generation can be performed in either an autoregressive (Kim et al., 2024; Pertsch et al., 2025) or a diffusion-based manner (Black et al., 2024; Bjorck et al., 2025), conditioning on the VLM features. We describe the detailed action generation process in Appendix F.

162 2.2 CONTEXTVLA
163

164 To leverage past observations for action generation, ContextVLA uses Vision-Language Model
165 (VLM) to process multi-frame observations. However, video inputs contain many tokens, sub-
166 stantially increasing compute and memory overhead in the VLM. To address this, our key idea is
167 to compress past observations into a single context token, allowing the VLM to capture the tem-
168 poral context of past observations, *e.g.*, movement of the robot, while reducing computation and
169 memory overhead. Specifically, we compress the past observations at the intermediate layer of the
170 VLM backbone by applying average pooling. And then, an action decoder generates robot actions
171 conditioned on the resulting VLM features.

172 Formally, given multi-frame observations $\mathbf{o}_{t-k:t}$, we first process them all through a vision encoder
173 f to obtain visual features $\mathbf{e}_{t-k:t} = f(\mathbf{o}_{t-k:t})$. We then use $\mathbf{x} = [\mathbf{e}_{t-k:t}, \mathbf{c}_t]$ *i.e.*, a concatenation of
174 $\mathbf{e}_{t-k:t}$ and \mathbf{c}_t , as input tokens to the VLM backbone g .

175
176
177 **Amortization of Past Observation.** The next step is to process the input tokens \mathbf{x} with the VLM
178 backbone g to extract the features that will be used to generate the action. To efficiently process
179 multi-frame observations using the VLM backbone, we compress past observations into a single
180 context token within the intermediate layer of the VLM model g .

181 Formally, let N be the number of VLM backbone blocks. We split the VLM backbone into two
182 parts at the n -th block. First, in the first n blocks, we process all tokens of \mathbf{x} through the VLM
183 blocks to get intermediate hidden states $\mathbf{h} = [\mathbf{h}_{t-k:t}, \mathbf{h}_c]$. In particular, when tokens are fed into the
184 self-attention layers, we apply a causal mask to the visual tokens, regardless of the original VLM
185 attention mask. This allows efficient inference by processing and caching past observations before
186 the next timestep. After this, we compress the past visual observations into a context token using
187 average pooling, *i.e.*, $\mathbf{m} = \text{AvgPool}([\mathbf{h}_{t-k:t-1}])$ to capture temporal context of past observations.
188 In the remaining $N - n$ blocks, we replace the hidden states of the past observations $\mathbf{h}_{t-k:t-1}$ with
189 the context token \mathbf{m} , and process $[\mathbf{m}, \mathbf{h}_t, \mathbf{h}_c]$ through the blocks. As a result, we obtain the VLM
190 features, which encode both the current observation and an amortized context of past observations.

191
192 **Action Decoder.** Our action decoder generates a chunk of robot action $\mathbf{a}_{t:t+l}$ with a length $l + 1$
193 ([Zhao et al., 2023](#); [Chi et al., 2023](#)), using VLM features as conditioning. Because our amortization
194 scheme does not depend on the type of action decoders, ContextVLA can be applied to any VLAs
195 regardless of their action decoder models. Specifically, it can be applied to autoregressive ([Kim
et al., 2024](#); [Bu et al., 2025b](#); [Pertsch et al., 2025](#)) or diffusion-based action decoders ([Black et al.,
2024](#); [Bjorck et al., 2025](#); [GEAR, 2025](#)). For instance, for the autoregressive modeling, we encode
196 an action $\mathbf{a}_{t:t+l}$ into discrete action tokens using the action tokenizer ([Bu et al., 2025b](#); [Pertsch
et al., 2025](#)), and then use the same VLM backbone to generate the discrete action tokens via next
197 action token prediction. For the diffusion-based modeling, we generate an action using a diffusion
198 transformer ([DiT Peebles & Xie \(2022\)](#)) conditioning on the VLM hidden states, *e.g.*, output tokens
199 of the VLM or key-values in the VLM blocks.

200
201
202 **Training Objective.** We train ContextVLA to predict the target ground-truth action $\mathbf{a}_{t:t+l}$ in the
203 expert trajectory $\tau = \{(\mathbf{o}_t, \mathbf{c}_t, \mathbf{a}_t)\}_{t=1}^T$. Specifically, we train the model π_θ to minimize the loss
204 $\ell(\pi_\theta(\mathbf{o}_{t-k:t}, \mathbf{c}_t), \mathbf{a}_{t:t+l})$, where ℓ corresponds to either a next-token prediction loss for the autore-
205 gressive action modeling or a flow-matching loss for the diffusion-based action modeling.

206
207
208 **Efficient Inference via KV-caching.** ContextVLA generates actions faster than a VLA that uses
209 videos without compression, since we use an amortized token instead of past observations in most
210 VLM blocks. In addition to this, we further make an inference of ContextVLA faster by processing
211 as many of the observations as possible before the next timestep. Specifically, at timestep $t - 1$,
212 we process $\mathbf{o}_{t-k:t-1}$ through the first n VLM blocks to obtain a KV-cache for each block, and
213 obtain a context token \mathbf{m} . At timestep t , since we explicitly implement the attention layers of the
214 first n VLM blocks with causal-attention, we generate actions using \mathbf{o}_t , pre-computed \mathbf{m} , and the
215 KV-cache, rather than re-processing $\mathbf{o}_{t-k:t-1}$.

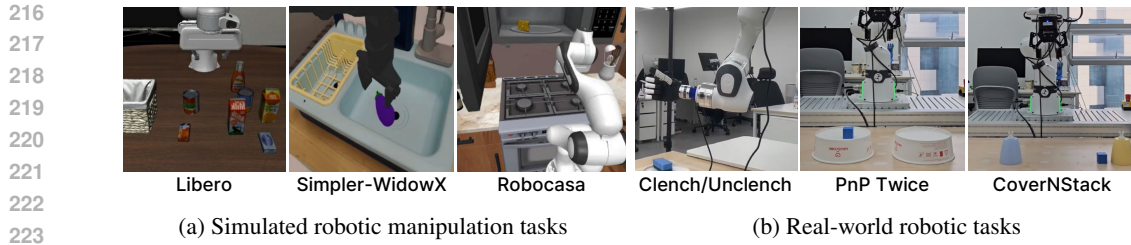


Figure 4: **Examples of visual observations from the evaluation tasks.** (a) We consider simulated robotic manipulation tasks from Libero (Liu et al., 2023a), Simpler-WidowX (Li et al., 2024b), and Robocasa (Nasiriany et al., 2024). (b) We design real-world robotic tasks: Clench/unclench hand (Clench/Unclench), pick-and-place twice (PnP Twice), and cover and stack (CoverNStack).

3 EXPERIMENTS

We design experiments to investigate the following questions:

- Can ContextVLA leverage the multi-frame observations to perform diverse robotic tasks without performance degradation? (Tables 1 to 3) In particular, is ContextVLA effective on robotic tasks that particularly need past observations? (Table 4)
- Is ContextVLA efficient during training and inference? (Table 5 and Figure 5)
- What is the effect of each component of ContextVLA? (Table 6)

3.1 EXPERIMENTAL SETUP

Implementation Details. We report the performance of our method, ContextVLA, by fine-tuning pre-trained Vision-Language-Action models (VLA). Specifically, we use π_0 (Black et al., 2024), GR00T N1.5 (GEAR, 2025), and π_0 -FAST (Pertsch et al., 2025) by following their official implementation. For π_0 and π_0 -FAST, we perform full-finetuning, *i.e.*, we update all model parameters, but we freeze the vision encoder and VLM backbone for GR00T N1.5. We use 8 consecutive frames as multi-frame observations, and we compress past observations into context tokens at the output of the 2nd VLM block (*i.e.*, $n=2$). We report the best performance by evaluating the models at fixed intervals during training. We provide more detailed implementation details in Appendix A.

Pre-training Details. We also report the performance of ContextVLA by fine-tuning ContextVLA pre-trained on the OXE Magic Soup dataset (O’Neill et al., 2024; Kim et al., 2024). We initialize the model from Qwen2.5VL 3B (Bai et al., 2025) and pre-train it to generate discrete action tokens using the FAST tokenizer (Pertsch et al., 2025). We pre-train our model for 180K iterations, using the AdamW optimizer with a batch size of 128.

Baselines. We compare the performance of ContextVLA with recent open-source VLAs: Octo (Team et al., 2024), OpenVLA (O’Neill et al., 2024), RoboVLMs (Liu et al., 2025), TraceVLA (Zheng et al., 2024), SpatialVLA (Qu et al., 2025), NORA (Hung et al., 2025), π_0 (Black et al., 2024), GR00T N1.5 (GEAR, 2025), and π_0 -FAST (Pertsch et al., 2025). In particular, to evaluate the benefit of ContextVLA, we compare π_0 , GR00T N1.5, and π_0 -FAST trained and fine-tuned with single-frame inputs against their counterparts fine-tuned with multi-frame inputs using our method. All models are fine-tuned with the same batch size and number of iterations, and we report their best success rates at fixed evaluation intervals. We describe more details of baselines in Appendix C.

3.2 SIMULATED ROBOTIC TASKS

To demonstrate our method can leverage multi-frame visual observations, we first evaluate our method by fine-tuning pre-trained VLAs on diverse simulated robotic manipulation benchmarks (see Figure 4a for examples of tasks from the benchmarks used in our experiments).

270
 271 **Table 1: Results on Libero.** We report the success rates (%) of various VLAs fine-tuned on the
 272 training dataset of Libero (Liu et al., 2023a; Kim et al., 2024). For π_0 (Black et al., 2024), π_0 -
 273 FAST (Pertsch et al., 2025), and GR00T N1.5 (GEAR, 2025), we report the performance with a
 274 standard deviation of 3 random training seeds by fine-tuning the pre-trained model with the official
 275 implementations, and other reported numbers borrow from Team et al. (2024); Hung et al. (2025).

Method	# frames	Spatial	Object	Goal	Long	Avg.
<i>VLAs pretrained on OXE dataset (O'Neill et al., 2024)</i>						
Octo (Team et al., 2024)	2	78.9	85.7	84.6	51.1	75.1
OpenVLA (Kim et al., 2024)	1	84.9	88.4	79.2	53.7	76.5
TraceVLA (Zheng et al., 2024)	6	84.9	85.2	75.1	54.1	74.8
SpatialVLA (Qu et al., 2025)	1	88.2	89.9	78.6	55.5	78.1
NORA (Hung et al., 2025)	1	92.2	95.4	89.4	74.6	87.9
ContextVLA (Ours)	8	95.8	99.2	92.6	87.0	93.7
<i>VLAs pretrained on external datasets</i>						
π_0 (Black et al., 2024)	1	96.3 \pm 0.3	97.3 \pm 0.4	96.2 \pm 0.3	88.8 \pm 0.3	94.7 \pm 0.1
+ ContextVLA (Ours)	8	97.9\pm0.5	98.9\pm0.6	96.3\pm0.3	93.1\pm0.6	96.6\pm0.1
π_0 -FAST (Pertsch et al., 2025)	1	96.3 \pm 1.1	97.5 \pm 0.9	94.5 \pm 0.6	84.8 \pm 1.4	93.3 \pm 0.5
+ ContextVLA (Ours)	8	97.8\pm0.6	98.9\pm0.4	95.9\pm0.6	90.8\pm0.9	95.8\pm0.2
GR00T N1.5 (GEAR, 2025)	1	98.0 \pm 0.5	99.3\pm0.2	96.9 \pm 0.3	88.7 \pm 0.8	95.7 \pm 0.2
+ ContextVLA (Ours)	8	98.6\pm0.2	99.1 \pm 0.2	97.3\pm0.1	93.0\pm0.3	97.0\pm0.1

291
 292 **Table 2: Results on Simpler-WidowX.** We report the success rates (%) of various VLAs fine-tuned
 293 on the Bridgev2 dataset (Walke et al., 2023). For π_0 (Black et al., 2024), π_0 -FAST (Pertsch et al.,
 294 2025), and GR00T N1.5 (GEAR, 2025), we report the performance with a standard deviation of 3
 295 random training seeds by fine-tuning the pre-trained model with the official implementations, and
 296 other reported numbers borrow from Qu et al. (2025).

Method	# frames	Spoon on Towel	Carrot on Plate	Stack Cube	Put Eggplant in Basket	Avg.
<i>VLAs pretrained on OXE dataset (O'Neill et al., 2024)</i>						
Octo-base (Team et al., 2024)	2	12.5	8.3	0.0	43.1	16.0
Octo-small (Team et al., 2024)	2	47.2	9.7	4.2	56.9	29.5
OpenVLA (Kim et al., 2024)	1	0.0	0.0	0.0	4.1	1.0
RoboVLMs (Liu et al., 2025)	16	29.2	25.0	12.5	58.3	31.3
SpatialVLA (Qu et al., 2025)	1	16.7	25.0	29.2	100.0	42.7
ContextVLA (Ours)	8	52.0	56.0	58.0	72.0	59.5
<i>VLAs pretrained on external datasets</i>						
π_0 (Black et al., 2024)	1	46.7 \pm 3.3	38.7 \pm 7.1	42.7\pm3.3	39.3 \pm 8.4	41.8 \pm 3.2
+ ContextVLA (Ours)	8	53.3\pm1.8	56.0\pm2.3	41.3 \pm 2.7	74.0\pm7.2	56.2\pm1.8
π_0 -FAST (Pertsch et al., 2025)	1	59.0 \pm 1.2	79.0 \pm 1.2	65.0 \pm 1.9	33.0 \pm 1.0	59.0 \pm 0.7
+ ContextVLA (Ours)	8	60.7\pm1.5	81.3\pm5.4	78.7\pm4.3	62.0\pm2.9	70.7\pm1.7
GR00T N1.5 (GEAR, 2025)	1	30.0\pm1.2	28.0 \pm 1.2	16.0\pm3.5	42.7 \pm 1.8	29.2 \pm 0.9
+ ContextVLA (Ours)	8	28.0 \pm 2.3	29.3\pm0.7	14.7 \pm 3.3	50.3\pm2.4	31.8\pm1.5

313
 314 **Experimental Setup.** We first consider Libero benchmark (Liu et al., 2023a), one of the popular
 315 benchmarks for evaluating VLA, which includes 4 different sub-benchmarks (Spatial, Object, Goal,
 316 and Long) that contain 10 tasks each. We also consider 4 tasks from the Simpler-WidowX bench-
 317 mark (Li et al., 2024b), which is a more challenging setup due to a visual gap between real-world
 318 training data and simulated test environments (Real-to-Sim). We report the performance by fine-
 319 tuning the models on Bridge v2 dataset (Ebert et al., 2021). Moreover, we consider the Robocasa
 320 benchmark (Nasiriany et al., 2024), which includes 24 tasks in simulated kitchen environments. It
 321 consists of more than 2500 different kitchen scenes across more than 150 object categories, requir-
 322 ing a policy to have instruction following and generalization ability over the scene and object. We
 323 report the performance by fine-tuning all models on the machine-generated training dataset, consist-
 324 ing of 100 demos per task. We provide a more detailed experimental setup in Appendix A and an
 325 explanation about the benchmark with evaluation details in Appendix B.1.

324
 325 **Table 3: Results on Robocasa.** We report the success rates (%) of various VLAs fine-tuned on the
 326 training dataset of Robocasa (Nasiriany et al., 2024), consisting of 24 tasks with 100 demos per task.
 327 We report the performance **with a standard deviation of 3 random training seeds** by fine-tuning the
 328 pre-trained model with the official implementations.

Method	# frames	Pick and Place	Others	Avg.
π_0 (Black et al., 2024)	1	32.9 \pm 0.4	70.3 \pm 1.4	57.9 \pm 0.9
+ ContextVLA (Ours)	8	35.6\pm0.8	70.4\pm0.2	58.8\pm0.2
π_0 -FAST (Pertsch et al., 2025)	1	46.1 \pm 1.0	68.1 \pm 0.8	60.3 \pm 0.1
+ ContextVLA (Ours)	8	48.6\pm0.6	68.7\pm0.6	62.0\pm0.2
GR00T N1.5 (GEAR, 2025)	1	51.8 \pm 1.4	67.6 \pm 1.1	62.3 \pm 0.3
+ ContextVLA (Ours)	8	52.8\pm0.5	70.2\pm0.5	64.4\pm0.2

336
 337 **Table 4: Results on real-world robotic tasks.** We report the success rates (%) of various VLAs fine-
 338 tuned on the training dataset of each task. We report the performance by fine-tuning the pre-trained
 339 model with the official implementations.

Method	# frames	Clench/Unclench	PnP Twice		CoverNStack	
			PnP Once	Full	Cover Cube	Full
π_0 (Black et al., 2024)	1	40.0	55.0	25.0	60.0	45.0
π_0 (Black et al., 2024)	8	40.0	60.0	55.0	65.0	45.0
+ ContextVLA (Ours)	8	80.0	75.0	65.0	85.0	60.0
GR00T N1.5 (Bjorck et al., 2025)	1	20.0	55.0	15.0	50.0	10.0
GR00T N1.5 (Bjorck et al., 2025)	8	80.0	60.0	30.0	50.0	25.0
+ ContextVLA (Ours)	8	80.0	70.0	50.0	55.0	35.0

349 **Results.** We find that our framework consistently improves the baselines as shown in Tables 1 to 3.
 350 This demonstrates that our method indeed can leverage multi-frame visual observations to generate
 351 action. Specifically, we first find that **ContextVLA**, pretrained on the OXE dataset, outperforms the
 352 **video-based VLAs**, demonstrating the effectiveness of **ContextVLA** over other multi-frame-based
 353 approaches (see Tables 1 and 2). We also observe that ContextVLA improves the baselines by a
 354 significant margin in Simpler-WidowX Benchmark (Table 2), a challenging setup due to the Real-
 355 to-Sim gap. For instance, ContextVLA improves the averaged success rates of π_0 by 14.6% (41.8%
 356 \rightarrow 56.2%). In addition, our framework improves the performance in the Robocasa Benchmark
 357 (Table 3). In particular, we observe that our framework improves the performance in Pick and Place
 358 (PnP) tasks, consisting of diverse target objects and positions. For instance, ContextVLA improves
 359 the averaged success rates of π_0 in PnP by 2.7% (32.9% \rightarrow 35.6%). This demonstrates that the
 360 performance gains with ContextVLA are not specific to the training setup, but instead highlight its
 361 ability to generalize across diverse objects and locations.

3.3 REAL-WORLD ROBOTIC TASKS

362 To investigate whether our method can leverage multi-frame visual observations, we further evaluate
 363 our method on real-world robotic tasks that require temporal context to perform the task successfully
 364 (see Figure 4b for examples of tasks used in our experiments).

365 **Tasks.** We design several real-world robotic tasks as follows (see Appendix B.2 for more details):

- 366 • **Clench/Unclench.** The policy should clench and unclench hand of the humanoid robot repeatedly.
 367 At an intermediate state between clenching and unclenching, it must decide to grasp or release the
 368 hand depending on the previous movement.
- 369 • **PnP Twice.** Given a cube and two plates (A and B), the policy should move the cube from plate
 370 A to B and then back from B to A. At each step, it must decide (a) whether to close the gripper
 371 (pick) or open it (place), and (b) which plate to place the cube on, based on the previous action.
- 372 • **CoverNStack.** Given a cube and two cups, the policy should cover the cube with the closest cup,
 373 and then stack the other cup on top of the covered cup. After covering the object with a cup, it must
 374 decide which cup to grasp and place it on top of the other cup, depending on the last movement.

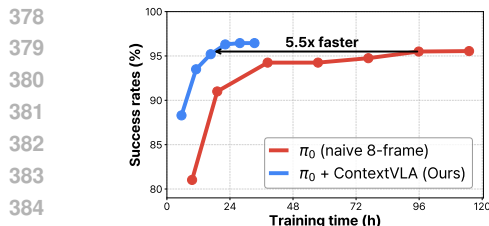


Figure 5: **Training efficiency.** We report the wall clock time of fine-tuning π_0 on Libero (Liu et al., 2023a) using 4 NVIDIA A100 80GB GPU.

Table 5: **Inference efficiency.** We report inference time (ms) required for π_0 (Black et al., 2024) to generate action from 8-frame, 2-view observations using a single NVIDIA A100 80GB GPU.

Compression	KV-caching	Time (ms)
✗	-	227.2
✓	✗	129.9
✓	✓	96.3

Table 6: **Component-wise analysis** on Libero (Liu et al., 2023a) and Simpler-WidowX (Li et al., 2024b) benchmarks. All models are π_0 (Black et al., 2024) fine-tuned for 60K iterations with a batch size of 32, using the Libero training dataset for Libero and the BridgeV2 dataset (Ebert et al., 2021) for Simpler-WidowX. We report the averaged success rates (%) of the models on each benchmark.

# frames	Depth	Context Token	Libero	Simpler-WidowX
1	π_0 (Black et al., 2024)	✓	94.6	41.8
8	π_0 (Black et al., 2024)	✓	95.6	47.8
2	2	✓	94.8	50.5
4	2	✓	95.0	52.0
8	2	✓	96.5	56.2
8	1	✓	96.1	46.5
8	2	✓	96.5	56.2
8	4	✓	96.4	53.5
8	6	✓	95.8	51.5
8	8	✓	96.4	48.5
8	2	✗	95.6	49.0
8	2	✓	96.5	56.2

Training and Evaluation Setup. For each task, we collect 50 demonstrations and report the performance by fine-tuning π_0 (Black et al., 2024) and GR00T N1.5 (GEAR, 2025) using our framework on the collected demonstrations. We train all models for 30K iterations using the AdamW optimizer with a batch size of 32. We evaluate each model with 20 trials per task and report partial (performs single time for repetitive tasks, and completes only the first subtask for long-horizon tasks) and full success rates. We describe the details of the evaluation in Appendix B.2.

Results. In Table 4, we find that ContextVLA improves the performance of the baselines by a significant margin. While single-frame baselines often fail to perform simple repetitive actions, e.g., clench/unclench, ContextVLA consistently outperforms them. This indicates that ContextVLA leverages temporal context to resolve temporal ambiguities. We observe the same results in sequential tasks (PnP Twice and CoverNStack), e.g., ContextVLA achieves the highest success rates on both tasks, but single-frame baselines often succeed partially. This further demonstrates the effectiveness of ContextVLA on long-horizon tasks that require temporal understanding. In particular, our framework even outperforms VLAs that utilize 8-frame observations without compression. For instance, in the CoverNStack tasks, fine-tuning π_0 with ContextVLA gets a 60% success rate, whereas fine-tuning it with 8-frame observations without compression gets 45%. The improvement can be attributed to the faster inference speed of our framework, as latency is known to degrade performance during real-world robot deployment (Black et al., 2025). This highlights the benefit of our approach that compresses the past observations. We provide the qualitative results in Appendix I.

3.4 ANALYSIS AND ABLATION STUDY

We first perform efficiency analysis in Figure 5 and Table 5. After that, in Table 6, we provide ablation studies to investigate the effect of each component of ContextVLA. [We include more analysis about the amortized context tokens in the Appendix E.](#)

Training Efficiency. In Figure 5, we analyze how efficient our compression scheme makes VLA when training using multi-frame observations. We compare the success rates under the same training wall-clock time with π_0 that uses 8-frame visual observations. We find that our framework is much faster to achieve the best performance of the π_0 , e.g., $5.5 \times$ faster on the Libero dataset.

Inference Efficiency. In Table 5, we measure the inference time of our framework to evaluate the inference efficiency of our compression scheme with multi-frame observations. We find that our framework is $2.4 \times$ faster than π_0 with 8-frame visual observations without compression. In particular, the efficient inference scheme with KV-caching reduces latency by 33.6 ms.

432 **Number of Past Observations.** We investigate the scalability of ContextVLA with the number of
 433 past observations. We evaluate this by fine-tuning π_0 (Black et al., 2024) with ContextVLA using
 434 different numbers of frames from 2 to 8. We find that the success rates consistently increase as the
 435 number of past observations increases. For instance, using 4 frames achieves a success rate of 52.0%
 436 on the Simpler-WidowX benchmark, while using 8 frames achieves a success rate of 56.2%.

437
 438 **Depth for Token Compression.** We also investigate the appropriate depth n for compressing past
 439 observations. By fine-tuning π_0 with past observations compressed into a context token at different
 440 backbone depths, we find that compression at shallow blocks ($n = 2$) is the optimal choice, while
 441 compression at other depths still shows the performance improvement. We note that the compression
 442 at shallow block allows the model to enhance efficiency during training and inference (see Table 5
 443 and Figure 5).

444
 445 **Effect of Amortized Context Token.** We further investigate whether the compressed context to-
 446 ken indeed provides meaningful information to generate actions. To evaluate this, we fine-tune π_0
 447 by compressing past observations at a middle block and compare two variants: using the compressed
 448 tokens in the remaining blocks or discarding them. We find that using context token improves the
 449 performance by a large margin, *e.g.*, in Simpler-WidowX, 49.0% \rightarrow 56.2%. This demonstrates that
 450 the context token captures temporal context from past observations, enabling the policy to generate
 451 actions better. We also find that π_0 using context token even outperforms π_0 trained on 8-frame
 452 observations without compression. We hypothesize this is because the context token summarizes
 453 past observations and mitigates redundancy across consecutive frames.

4 RELATED WORK

454
 455
 456 **Vision-Language-Action Models (VLA).** Recently, VLAs (O’Neill et al., 2024; Zitkovich et al.,
 457 2023; Kim et al., 2024) have emerged as a promising framework for general robot policy that can per-
 458 form many different tasks with a single model, by leveraging pre-trained Vision-Language Model
 459 (VLM) (Liu et al., 2023b; Beyer et al., 2024; Bai et al., 2025; Chen et al., 2025) and training on
 460 large-scale robot manipulation datasets (Ebert et al., 2021; Walke et al., 2023; O’Neill et al., 2024;
 461 Khazatsky et al., 2024; Bu et al., 2025a). However, many existing VLAs are trained to process
 462 only a single-frame visual observation to generate actions (Kim et al., 2024; Li et al., 2024a; Black
 463 et al., 2024; Shukor et al., 2025; Yang et al., 2025; Bjorck et al., 2025; Hung et al., 2025; Qu et al.,
 464 2025; Driess et al., 2025; GEAR, 2025; Cheang et al., 2025), limiting their ability to perform diverse
 465 robotic tasks that require temporal context. To address this, several recent approaches have attempted
 466 to leverage multi-frame observations. A common strategy is to use full context of multi-frame ob-
 467 servations to generate actions (Wu et al., 2023; Team et al., 2024; Cheang et al., 2024; Huang et al.,
 468 2025; Liu et al., 2025; Wang et al., 2025). However, using multi-frame observations without com-
 469 pression increases computation and memory overheads by increasing input dimensionality that VLA
 470 processes, resulting in inefficient training and inference. In contrast, a recent approach, TraceVLA
 471 (Zheng et al., 2024), summarizes the observations by tracking the robot trace. However, it requires
 472 external point tracking model (Karaev et al., 2024), making inference still slow. In this paper, we
 473 introduce an efficient VLA framework that leverages multi-frame visual observations.

474
 475
 476 **Efficient Training and Inference of Multi-frame Policy.** A higher input dimensionality com-
 477 pared to single-frame observations makes the training and inference of policy model inefficient.
 478 This hinders scaling up the policy model training (Black et al., 2024; Bjorck et al., 2025), and poses
 479 a significant challenge for deployment, as inference speed is a critical issue in robotics (Black et al.,
 480 2025). To address this, some approaches handle multi-frame inputs efficiently by compressing past
 481 observations (Wen et al., 2020; Seo et al., 2023), selecting a key-frames (Wen et al., 2021), or sum-
 482 marizing entire sequences into high-level visualizations (Sundaresan et al., 2024; Zheng et al., 2024).
 483 In addition, recent work proposes two-stage scheme where it first trains a single-frame policy, and
 484 then trains a multi-frame policy after freezing visual encoder (Torne et al., 2025). Our work also
 485 proposes a method that allows the policy to leverage multi-frame observation more efficiently than
 compressing past observations into a single token.

486 **5 CONCLUSION**

487

488 In this work, we have presented ContextVLA, an efficient framework for Vision-Language-Action
 489 models (VLA) that leverages multi-frame visual observations for action generation. Motivated by
 490 the observation that VLAs mitigate the performance degradation suffered by behavior cloning poli-
 491 cies with multi-frame inputs, we introduce a simple yet effective method that compresses past obser-
 492 vations into a single context token, allowing the VLA to capture temporal context more efficiently.
 493 Our experiments show that ContextVLA leverages multi-frame observations to improve the per-
 494 formance of existing VLAs. We also find that our scheme retains the benefits of multi-frame training
 495 with less training and inference time. We hope that our work facilitates future research toward
 496 generalist robot policies that can capture temporal context to perform more diverse tasks.

497

498 **REPRODUCIBILITY STATEMENT**

499

500 For the reproducibility of our results, we provide the implementation details in Appendices **A** and **B**,
 501 including training and inference setups. In addition, we will open-source the source code with the
 502 model checkpoint.

503

504 **REFERENCES**

505

506 Nasir Ahmed, T. Natarajan, and Kamisetty R Rao. Discrete cosine transform. *IEEE transactions*
 507 *on Computers*, 2006.

508 Jean-Baptiste Alayrac, Jeff Donahue, Pauline Luc, Antoine Miech, Iain Barr, Yana Hasson, Karel
 509 Lenc, Arthur Mensch, Katherine Millican, Malcolm Reynolds, et al. Flamingo: a visual language
 510 model for few-shot learning. In *Advances in Neural Information Processing Systems*, 2022.

511 Shuai Bai, Keqin Chen, Xuejing Liu, Jialin Wang, Wenbin Ge, Sibo Song, Kai Dang, Peng Wang,
 512 Shijie Wang, Jun Tang, et al. Qwen2. 5-vl technical report. *arXiv preprint arXiv:2502.13923*,
 513 2025.

514 Mayank Bansal, Alex Krizhevsky, and Abhijit Ogale. Chauffeurnet: Learning to drive by imitating
 515 the best and synthesizing the worst. In *Robotics: Science and Systems*, 2019.

516 Lucas Beyer, Andreas Steiner, André Susano Pinto, Alexander Kolesnikov, Xiao Wang, Daniel Salz,
 517 Maxim Neumann, Ibrahim Alabdulmohsin, Michael Tschannen, Emanuele Bugliarello, et al.
 518 Paligemma: A versatile 3b vlm for transfer. *arXiv preprint arXiv:2407.07726*, 2024.

519 Johan Bjorck, Fernando Castañeda, Nikita Cherniakov, Xingye Da, Runyu Ding, Linxi Fan,
 520 Yu Fang, Dieter Fox, Fengyuan Hu, Spencer Huang, et al. Gr00t n1: An open foundation model
 521 for generalist humanoid robots. *arXiv preprint arXiv:2503.14734*, 2025.

522 Kevin Black, Noah Brown, Danny Driess, Adnan Esmail, Michael Equi, Chelsea Finn, Niccolo
 523 Fusai, Lachy Groom, Karol Hausman, Brian Ichter, et al. π_0 : A vision-language-action flow
 524 model for general robot control. *arXiv preprint arXiv:2410.24164*, 2024.

525 Kevin Black, Manuel Y Galliker, and Sergey Levine. Real-time execution of action chunking flow
 526 policies. *arXiv preprint arXiv:2506.07339*, 2025.

527 Qingwen Bu, Jisong Cai, Li Chen, Xiuqi Cui, Yan Ding, Siyuan Feng, Shenyuan Gao, Xindong
 528 He, Xuan Hu, Xu Huang, et al. Agibot world colosseo: A large-scale manipulation platform for
 529 scalable and intelligent embodied systems. *arXiv preprint arXiv:2503.06669*, 2025a.

530 Qingwen Bu, Yanting Yang, Jisong Cai, Shenyuan Gao, Guanghui Ren, Maoqing Yao, Ping Luo, and
 531 Hongyang Li. Univla: Learning to act anywhere with task-centric latent actions. *arXiv preprint*
 532 *arXiv:2505.06111*, 2025b.

533 Chi-Lam Cheang, Guangzeng Chen, Ya Jing, Tao Kong, Hang Li, Yifeng Li, Yuxiao Liu, Hongtao
 534 Wu, Jiafeng Xu, Yichu Yang, et al. Gr-2: A generative video-language-action model with web-
 535 scale knowledge for robot manipulation. *arXiv preprint arXiv:2410.06158*, 2024.

540 Chilam Cheang, Sijin Chen, Zhongren Cui, Yingdong Hu, Liqun Huang, Tao Kong, Hang Li, Yifeng
 541 Li, Yuxiao Liu, Xiao Ma, et al. Gr-3 technical report. *arXiv preprint arXiv:2507.15493*, 2025.
 542

543 Guo Chen, Zhiqi Li, Shihao Wang, Jindong Jiang, Yicheng Liu, Lidong Lu, De-An Huang, Wonmin
 544 Byeon, Matthieu Le, Tuomas Rintamaki, et al. Eagle 2.5: Boosting long-context post-training for
 545 frontier vision-language models. *arXiv preprint arXiv:2504.15271*, 2025.

546 Cheng Chi, Zhenjia Xu, Siyuan Feng, Eric Cousineau, Yilun Du, Benjamin Burchfiel, Russ Tedrake,
 547 and Shuran Song. Diffusion policy: Visuomotor policy learning via action diffusion. *The Inter-
 548 national Journal of Robotics Research*, 2023.

549

550 Felipe Codevilla, Eder Santana, Antonio M López, and Adrien Gaidon. Exploring the limitations of
 551 behavior cloning for autonomous driving. In *IEEE International Conference on Computer Vision*,
 552 2019.

553

554 Pim De Haan, Dinesh Jayaraman, and Sergey Levine. Causal confusion in imitation learning. In
 555 *Advances in Neural Information Processing Systems*, 2019.

556

557 Danny Driess, Jost Tobias Springenberg, Brian Ichter, Lili Yu, Adrian Li-Bell, Karl Pertsch, Allen Z
 558 Ren, Homer Walke, Quan Vuong, Lucy Xiaoyang Shi, et al. Knowledge insulating vision-
 559 language-action models: Train fast, run fast, generalize better. *arXiv preprint arXiv:2505.23705*,
 2025.

560

561 Frederik Ebert, Yanlai Yang, Karl Schmeckpeper, Bernadette Bucher, Georgios Georgakis, Kostas
 562 Daniilidis, Chelsea Finn, and Sergey Levine. Bridge data: Boosting generalization of robotic
 563 skills with cross-domain datasets. *arXiv preprint arXiv:2109.13396*, 2021.

564

565 Philip Gage. A new algorithm for data compression. *C Users Journal*, 1994.

566

567 NVIDIA GEAR. Gr00t n1.5: An improved open foundation model for generalist humanoid robots.
https://research.nvidia.com/labs/gear/gr00t-n1_5/, June 2025. Accessed:
 568 2025-09-09.

569

570 Huang Huang, Fangchen Liu, Letian Fu, Tingfan Wu, Mustafa Mukadam, Jitendra Malik, Ken Gold-
 571 berg, and Pieter Abbeel. Otter: A vision-language-action model with text-aware visual feature
 572 extraction. *arXiv preprint arXiv:2503.03734*, 2025.

573

574 Chia-Yu Hung, Qi Sun, Pengfei Hong, Amir Zadeh, Chuan Li, U Tan, Navonil Majumder, Soujanya
 575 Poria, et al. Nora: A small open-sourced generalist vision language action model for embodied
 576 tasks. *arXiv preprint arXiv:2504.19854*, 2025.

577

578 Vidhi Jain, Maria Attarian, Nikhil J Joshi, Ayzaan Wahid, Danny Driess, Quan Vuong, Pannag R
 579 Sanketi, Pierre Sermanet, Stefan Welker, Christine Chan, et al. Vid2robot: End-to-end video-
 580 conditioned policy learning with cross-attention transformers. In *Robotics: Science and Systems*,
 2024.

581

582 Leslie Pack Kaelbling, Michael L Littman, and Anthony R Cassandra. Planning and acting in
 583 partially observable stochastic domains. *Artificial intelligence*, 101(1-2):99–134, 1998.

584

585 Nikita Karaev, Ignacio Rocco, Benjamin Graham, Natalia Neverova, Andrea Vedaldi, and Christian
 586 Rupprecht. Cotracker: It is better to track together. In *European conference on computer vision*,
 587 pp. 18–35. Springer, 2024.

588

589 Alexander Khazatsky, Karl Pertsch, Suraj Nair, Ashwin Balakrishna, Sudeep Dasari, Siddharth
 590 Karamcheti, Soroush Nasiriany, Mohan Kumar Srirama, Lawrence Yunliang Chen, Kirsty El-
 591 lis, et al. Droid: A large-scale in-the-wild robot manipulation dataset. *arXiv preprint
 592 arXiv:2403.12945*, 2024.

593

Moo Jin Kim, Karl Pertsch, Siddharth Karamcheti, Ted Xiao, Ashwin Balakrishna, Suraj Nair,
 Rafael Rafailov, Ethan Foster, Grace Lam, Pannag Sanketi, et al. Openvla: An open-source
 594 vision-language-action model. *arXiv preprint arXiv:2406.09246*, 2024.

594 Hao Li, Shuai Yang, Yilun Chen, Yang Tian, Xiaoda Yang, Xinyi Chen, Hanqing Wang, Tai Wang,
 595 Feng Zhao, Dahua Lin, et al. Cronusvla: Transferring latent motion across time for multi-frame
 596 prediction in manipulation. *arXiv preprint arXiv:2506.19816*, 2025.

597

598 Qixiu Li, Yaobo Liang, Zeyu Wang, Lin Luo, Xi Chen, Mozheng Liao, Fangyun Wei, Yu Deng,
 599 Sicheng Xu, Yizhong Zhang, et al. Cogact: A foundational vision-language-action model for syn-
 600 ergizing cognition and action in robotic manipulation. *arXiv preprint arXiv:2411.19650*, 2024a.

601 Xuanlin Li, Kyle Hsu, Jiayuan Gu, Karl Pertsch, Oier Mees, Homer Rich Walke, Chuyuan Fu,
 602 Ishikaa Lunawat, Isabel Sieh, Sean Kirmani, et al. Evaluating real-world robot manipulation
 603 policies in simulation. *arXiv preprint arXiv:2405.05941*, 2024b.

604

605 Bo Liu, Yifeng Zhu, Chongkai Gao, Yihao Feng, Qiang Liu, Yuke Zhu, and Peter Stone. Libero:
 606 Benchmarking knowledge transfer for lifelong robot learning. In *Advances in Neural Information
 607 Processing Systems*, 2023a.

608

609 Haotian Liu, Chunyuan Li, Qingyang Wu, and Yong Jae Lee. Visual instruction tuning. In *Advances
 610 in Neural Information Processing Systems*, 2023b.

611

612 Huaping Liu, Xinghang Li, Peiyan Li, Minghuan Liu, Dong Wang, Jirong Liu, Bingyi Kang, Xiao
 613 Ma, Tao Kong, and Hanbo Zhang. Towards generalist robot policies: What matters in building
 614 vision-language-action models. *arXiv preprint arXiv:2412.14058*, 2025.

615

616 Ajay Mandlekar, Danfei Xu, Josiah Wong, Soroush Nasiriany, Chen Wang, Rohun Kulkarni, Li Fei-
 617 Fei, Silvio Savarese, Yuke Zhu, and Roberto Martín-Martín. What matters in learning from offline
 618 human demonstrations for robot manipulation. *arXiv preprint arXiv:2108.03298*, 2021.

619

620 Oier Mees, Lukas Hermann, Erick Rosete-Beas, and Wolfram Burgard. Calvin: A benchmark for
 621 language-conditioned policy learning for long-horizon robot manipulation tasks. *IEEE Robotics
 622 and Automation Letters*, 2022.

623

624 Urs Muller, Jan Ben, Eric Cosatto, Beat Flepp, and Yann Cun. Off-road obstacle avoidance through
 625 end-to-end learning. In *Advances in Neural Information Processing Systems*, 2005.

626

627 Soroush Nasiriany, Abhiram Maddukuri, Lance Zhang, Adeet Parikh, Aaron Lo, Abhishek Joshi,
 628 Ajay Mandlekar, and Yuke Zhu. Robocasa: Large-scale simulation of everyday tasks for gener-
 629 alist robots. In *Robotics: Science and Systems*, 2024.

630

631 Abby O'Neill, Abdul Rehman, Abhiram Maddukuri, Abhishek Gupta, Abhishek Padalkar, Abraham
 632 Lee, Acorn Pooley, Agrim Gupta, Ajay Mandlekar, Ajinky Jain, et al. Open x-embodiment:
 633 Robotic learning datasets and rt-x models: Open x-embodiment collaboration 0. In *2024 IEEE
 634 International Conference on Robotics and Automation (ICRA)*, 2024.

635

636 William Peebles and Saining Xie. Scalable diffusion models with transformers. In *IEEE Interna-
 637 tional Conference on Computer Vision*, 2022.

638

639 Karl Pertsch, Kyle Stachowicz, Brian Ichter, Danny Driess, Suraj Nair, Quan Vuong, Oier Mees,
 640 Chelsea Finn, and Sergey Levine. Fast: Efficient action tokenization for vision-language-action
 641 models. *arXiv preprint arXiv:2501.09747*, 2025.

642

643 Delin Qu, Haoming Song, Qizhi Chen, Yuanqi Yao, Xinyi Ye, Yan Ding, Zhigang Wang, JiaYuan
 644 Gu, Bin Zhao, Dong Wang, et al. Spatialvla: Exploring spatial representations for visual-
 645 language-action model. *arXiv preprint arXiv:2501.15830*, 2025.

646

647 Michael S Ryoo, Honglu Zhou, Shrikant Kendre, Can Qin, Le Xue, Manli Shu, Jongwoo Park,
 648 Kanchana Ranasinghe, Silvio Savarese, Ran Xu, et al. xgen-mm-vid (blip-3-video): You only
 649 need 32 tokens to represent a video even in vlms. In *Advances in Neural Information Processing
 650 Systems*, 2024.

651

652 Seokin Seo, HyeongJoo Hwang, Hongseok Yang, and Kee-Eung Kim. Regularized behavior cloning
 653 for blocking the leakage of past action information. In *Advances in Neural Information Processing
 654 Systems*, 2023.

648 Hao Shi, Bin Xie, Yingfei Liu, Lin Sun, Fengrong Liu, Tiancai Wang, Erjin Zhou, Haoqiang Fan,
 649 Xiangyu Zhang, and Gao Huang. Memoryvla: Perceptual-cognitive memory in vision-language-
 650 action models for robotic manipulation. *arXiv preprint arXiv:2508.19236*, 2025.

651

652 Mustafa Shukor, Dana Aubakirova, Francesco Capuano, Pepijn Kooijmans, Steven Palma,
 653 Adil Zouitine, Michel Aractingi, Caroline Pascal, Martino Russi, Andres Marafioti, et al.
 654 Smolvla: A vision-language-action model for affordable and efficient robotics. *arXiv preprint*
 655 *arXiv:2506.01844*, 2025.

656

657 Jonathan Spencer, Sanjiban Choudhury, Arun Venkatraman, Brian Ziebart, and J Andrew Bag-
 658 nell. Feedback in imitation learning: The three regimes of covariate shift. *arXiv preprint*
 659 *arXiv:2102.02872*, 2021.

660

661 Priya Sundaresan, Quan Vuong, Jiayuan Gu, Peng Xu, Ted Xiao, Sean Kirmani, Tianhe Yu, Michael
 662 Stark, Ajinkya Jain, Karol Hausman, et al. Rt-sketch: Goal-conditioned imitation learning from
 663 hand-drawn sketches. In *8th Annual Conference on Robot Learning*, 2024.

664

665 Octo Model Team, Dibya Ghosh, Homer Walke, Karl Pertsch, Kevin Black, Oier Mees, Sudeep
 666 Dasari, Joey Hejna, Tobias Kreiman, Charles Xu, et al. Octo: An open-source generalist robot
 667 policy. *arXiv preprint arXiv:2405.12213*, 2024.

668

669 Marcel Torne, Andy Tang, Yuejiang Liu, and Chelsea Finn. Learning long-context diffusion policies
 670 via past-token prediction. *arXiv preprint arXiv:2505.09561*, 2025.

671

672 Michael Tschannen, Alexey Gritsenko, Xiao Wang, Muhammad Ferjad Naeem, Ibrahim Alabdul-
 673 mohsin, Nikhil Parthasarathy, Talfan Evans, Lucas Beyer, Ye Xia, Basil Mustafa, et al. Siglip 2:
 674 Multilingual vision-language encoders with improved semantic understanding, localization, and
 675 dense features. *arXiv preprint arXiv:2502.14786*, 2025.

676

677 Homer Rich Walke, Kevin Black, Tony Z Zhao, Quan Vuong, Chongyi Zheng, Philippe Hansen-
 678 Estruch, Andre Wang He, Vivek Myers, Moo Jin Kim, Max Du, et al. Bridgedata v2: A dataset
 679 for robot learning at scale. In *Conference on Robot Learning*, 2023.

680

681 Dequan Wang, Coline Devin, Qi-Zhi Cai, Philipp Krähenbühl, and Trevor Darrell. Monocular plan
 682 view networks for autonomous driving. In *IEEE/RSJ International Conference on Intelligent*
 683 *Robots and Systems*, 2019.

684

685 Yuqi Wang, Xinghang Li, Wenxuan Wang, Junbo Zhang, Yingyan Li, Yuntao Chen, Xinlong Wang,
 686 and Zhaoxiang Zhang. Unified vision-language-action model. *arXiv preprint arXiv:2506.19850*,
 687 2025.

688

689 Chuan Wen, Jierui Lin, Trevor Darrell, Dinesh Jayaraman, and Yang Gao. Fighting copycat agents
 690 in behavioral cloning from observation histories. In *Advances in Neural Information Processing*
 691 *Systems*, 2020.

692

693 Chuan Wen, Jierui Lin, Jianing Qian, Yang Gao, and Dinesh Jayaraman. Keyframe-focused visual
 694 imitation learning. *arXiv preprint arXiv:2106.06452*, 2021.

695

696 Hongtao Wu, Ya Jing, Chilam Cheang, Guangzeng Chen, Jiafeng Xu, Xinghang Li, Minghuan Liu,
 697 Hang Li, and Tao Kong. Unleashing large-scale video generative pre-training for visual robot
 698 manipulation. *arXiv preprint arXiv:2312.13139*, 2023.

699

700 Jianwei Yang, Reuben Tan, Qianhui Wu, Ruijie Zheng, Baolin Peng, Yongyuan Liang, Yu Gu,
 701 Mu Cai, Seonghyeon Ye, Joel Jang, et al. Magma: A foundation model for multimodal ai agents.
 702 In *IEEE Conference on Computer Vision and Pattern Recognition*, 2025.

703

704 Xiaohua Zhai, Basil Mustafa, Alexander Kolesnikov, and Lucas Beyer. Sigmoid loss for language
 705 image pre-training. In *IEEE Conference on Computer Vision and Pattern Recognition*, 2023.

706

707 Jiazhao Zhang, Kunyu Wang, Shaoan Wang, Minghan Li, Haoran Liu, Songlin Wei, Zhongyuan
 708 Wang, Zhizheng Zhang, and He Wang. Uni-navid: A video-based vision-language-action model
 709 for unifying embodied navigation tasks. In *Robotics: Science and Systems*, 2025.

702 Tony Z Zhao, Vikash Kumar, Sergey Levine, and Chelsea Finn. Learning fine-grained bimanual
703 manipulation with low-cost hardware. *arXiv preprint arXiv:2304.13705*, 2023.

704
705 Ruijie Zheng, Yongyuan Liang, Shuaiyi Huang, Jianfeng Gao, Hal Daumé III, Andrey Kolobov,
706 Furong Huang, and Jianwei Yang. Tracevla: Visual trace prompting enhances spatial-temporal
707 awareness for generalist robotic policies. *arXiv preprint arXiv:2412.10345*, 2024.

708 Brianna Zitkovich, Tianhe Yu, Sichun Xu, Peng Xu, Ted Xiao, Fei Xia, Jialin Wu, Paul Wohlhart,
709 Stefan Welker, Ayzaan Wahid, et al. Rt-2: Vision-language-action models transfer web knowledge
710 to robotic control. In *Conference on Robot Learning*, 2023.

711

712

713

714

715

716

717

718

719

720

721

722

723

724

725

726

727

728

729

730

731

732

733

734

735

736

737

738

739

740

741

742

743

744

745

746

747

748

749

750

751

752

753

754

755

756 **A IMPLEMENTATION DETAILS**
757

758 We report the performance of ContextVLA, by fine-tuning pre-trained Vision-Language-Action
 759 models (VLA). Specifically, we use π_0 (Black et al., 2024), GR00T N1.5 (Bjorck et al., 2025),
 760 and π_0 -FAST (Pertsch et al., 2025) by following their official implementation: **For π_0 and π_0 -FAST,
 761 we fine-tune all model parameters, and for GR00T N1.5, we freezes vision encoder and VLM back-
 762 bones.** We use 8 consecutive frames as multi-frame observations, and we compress past observations
 763 into context tokens at the output of the 2nd VLM block (*i.e.*, $n=2$). **For simulated tasks, we train π_0 +
 764 ContextVLA, GR00T N1.5 + ContextVLA for 60K iterations, but train π_0 -FAST + ContextVLA for
 765 30K iterations as π_0 -FAST converges faster than π_0 and GR00T N1.5 (Pertsch et al., 2025).** For
 766 real-world tasks, we only need to train the model on a single task with 50 demonstrations, so we
 767 train π_0 + ContextVLA and GR00T N1.5 + ContextVLA for fewer (30K) iterations.

768 Table 7: Hyperparameter details of training ContextVLA in simulated robotic tasks

	π_0 + ContextVLA	π_0 -FAST + ContextVLA	GR00T N1.5 + ContextVLA
optimizer	AdamW	AdamW	AdamW
optimizer momentum	$\beta_1, \beta_2 = 0.9, 0.95$	$\beta_1, \beta_2 = 0.9, 0.95$	$\beta_1, \beta_2 = 0.95, 0.999$
optimizer weight decay	1e-10	1e-10	1e-5
learning rate	2.5e-5	2.5e-5	1e-4
learning rate scheduler	Cosine decay	Cosine decay	Cosine decay
warmup iterations	1000	1000	3000
batch size	32	32	32
training iterations (simulated tasks)	60000	30000	60000
training iterations (real-world tasks)	30000	-	30000

779 **B BENCHMARK DETAILS**
780781 **B.1 SIMULATED ROBOTIC MANIPULATION BENCHMARKS**
782

783 We evaluate our method on the following simulated robotic manipulation benchmarks.
784

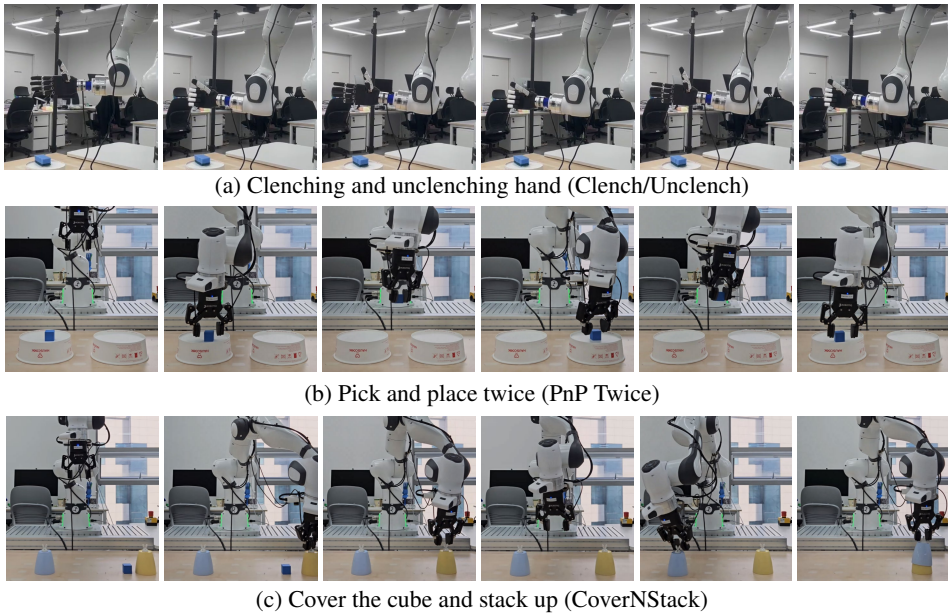
785 **Libero.** We consider Libero benchmark (Liu et al., 2023a), a widely used simulated robotic
 786 manipulation benchmark for evaluating the performance of Vision-Language-Action models (VLA). It
 787 uses a Franka robot. It consists of 4 different sub-benchmarks (Spatial, Object, Goal, and Long),
 788 each comprising 10 tasks. Among them, the tasks in the Libero-Long consist of 2 sequential sub-
 789 tasks, where the appropriate next action depends on whether the previous step has been completed
 790 or not. In addition, many tasks in Libero-Spatial, Object, Goal benchmark are simple, short-horizon
 791 pick-and-place with multi-view camera setups, which can be used to evaluate whether multi-frame
 792 observations do not degrade performance in Markovian tasks. While each sub-benchmark has its
 793 own training dataset (Team et al., 2024; Kim et al., 2024), we follow the setup of π_0 (Black et al.,
 794 2024) that combines all training datasets to train the models and reports the performance separately
 795 for each sub-benchmark. We use a fixed front-view camera and a wrist camera of 224×224 resolu-
 796 tion without depth. We use the end-effector position as the action mode. **We train our method on
 797 the combined training dataset of Libero with 3 random seeds, evaluate each model 50 times for each
 798 task by varying the position of objects, and report the average success rates with a 95% confidence
 799 interval.**

800 **Simpler-WidowX.** We consider Simpler-WidowX Benchmark (Li et al., 2024b), a more challeng-
 801 ing simulated benchmark. It uses the WidowX robot. It consists of 4 tasks (Spoon on Towel, Carrot
 802 on Plate, Stack Cube, and Put Eggplant in Basket). We follow the common setup Li et al. (2024b)
 803 that uses the BridgeV2 dataset (Walke et al., 2023) to fine-tune the model, and then evaluate the
 804 models in this benchmark. We use the primary camera in the BridgeV2 dataset when training, and
 805 use a fixed third-person view camera of 224×224 resolution without depth. We use the end-effector
 806 position as the action mode. **Here, because the policy uses only a third-person view, which leads
 807 to partial observability as some parts of the robot arm often move outside the camera, and objects
 808 become occluded during manipulation. We train our method on the BridgeV2 dataset with 3 random
 809 seeds, and evaluate each model 50 times for each task by varying the random seed of this benchmark,
 and report the average success rates with a 95% confidence interval.**

810 **Robocasa.** We additionally consider Robocasa benchmark (Nasiriany et al., 2024), which includes
 811 24 tasks in simulated kitchen environments. We randomly sample 100 demonstrations per task in the
 812 machine-generated training dataset in Robocasa and combine all these demonstrations to train the
 813 models. We use a fixed left-view camera, a fixed right-view camera, and a wrist camera of 224×224
 814 resolution without depth. We use the end-effector position as the action mode. We train our method
 815 on the training dataset of Robocasa with 3 random seeds, evaluate models 50 times for each task
 816 with random seeds, and report the average success rates with a 95% confidence interval.
 817

818 B.2 REAL-WORLD ROBOTIC TASKS

819 We design several real-world robotic tasks. We collect 50 demonstrations per task and report the
 820 performance of the models by fine-tuning VLAs on each task. We evaluate models 20 times for
 821 each task. In the below, we describe the detailed setups (see Figure 6 for a visualization of the
 822 collected train demonstrations):
 823



824 Figure 6: **Visualization of real-world robotic task demonstrations.**

825 **Clench/Unclench.** The policy should clenched and unclenched the right hand of a humanoid robot
 826 repeatedly. For the robot setup, we use Franka Research 3 (Robot arm) + Inspire Dex hands RH56FTP
 827 (Robot hand). We use the third-person view camera and wrist camera of 224×224 resolution without
 828 depth. We use an absolute end-effector position as the action mode. We use the text instruction
 829 “*Clench and then unclenched the hand repeatedly.*” for this task. We report success if the robot clenched
 830 and unclenched a hand at least five times within 1 minute.
 831

832 **PnP Twice.** Given a cube and two plates (A and B), the policy should move the cube from plate A
 833 to B and then back from B to A. We use Franka Research 3 (Robot arm) + DROID gripper. We use
 834 the third-person view camera and wrist camera of 720×1280 resolution without depth. We use the
 835 visual observation after resizing it to 224×224 resolution. We use absolute joint position as action
 836 mode. We use the text instruction “*Pick up the cube and place it on the opposite side, and then
 837 return it to the original side.*” for this task. We report partial success if the robot move the cube to
 838 the opposite side once, and full success if the robot complete the task within 1 minute.
 839

840 **CoverNStack.** Given a cube and two cups, the policy should cover the cube with the closest cup,
 841 and then stack the other cup on top of the covered cup. We use the same robot, camera setup, and
 842 action mode as in the PnP Twice task. We use the text instruction “*Cover the cube with the nearest
 843 cup, then stack the other cup on top of it.*” for this task. We report partial success if the robot covers
 844 the cube, and full success if the robot complete the task within 1 minute.
 845

C BASELINES

We describe the main idea of baseline methods that we used for the evaluation.

- **Octo** (Team et al., 2024) processes visual observations and task instructions to produce a read-out token, which is fed into a diffusion model to generate actions.
- **OpenVLA** (Kim et al., 2024) fine-tunes a pretrained VLM to autoregressively generate action tokens from visual observations and task instructions.
- **RoboVLMs** (Liu et al., 2025) uses multi-frame observations to generate action. It obtains tokens from each frame via the VLM and then concatenates them to generate the action.
- **TraceVLA** (Zheng et al., 2024) first extracts an image of the robot trajectories from multi-frame observation using point tracking models, and then uses this image to generate action via autoregressive modeling.
- **SpatialVLA** (Qu et al., 2025) integrates 3D spatial understanding capability into VLAs by using Ego3D position encoding and adaptive action grids.
- **NORA** (Hung et al., 2025) uses Qwen2.5-VL (Bai et al., 2025) as a backbone model to generate discrete action tokens. It decodes the token to action values using the FAST tokenizer.
- π_0 (Black et al., 2024) proposes a diffusion-based VLA that shares self-attention layers between VLM and diffusion transformer.
- π_0 -**FAST** (Pertsch et al., 2025) is an autoregressive VLA utilizing Frequency-space Action Sequence Tokenization (FAST) action tokenizer. The tokenizer applies the discrete cosine transform (DCT) algorithm for encoding the continuous action values to discrete tokens. Then, the FAST tokenizer applies Byte Pair Encoding (BPE) to compress sequences.
- **GR00T N1.5** (GEAR, 2025) also proposes diffusion-based VLA, but it feeds the last hidden states of the VLM into the cross-attention layer of the diffusion transformer.

D RESULTS ON CALVIN BENCHMARK

To demonstrate that our method can perform long-horizon tasks, we evaluate our method by fine-tuning pre-trained VLAs on the CALVIN (ABC→D) benchmark.

Setup. CALVIN (ABC→D) benchmark (Mees et al., 2022) is a simulated robotic manipulation benchmark designed to evaluate the ability of policy in a zero-shot long-horizon task. It consists of 34 distinct tasks. We train both π_0 and $\pi_0 + \text{ContextVLA}$ on the training dataset collected from environments A, B, and C for 60K iterations with a batch size of 32. We then evaluate each model on the environment D with 1000 trials and report the average number of successes among 5 sequential subtasks.

Results. As shown in Table 8, ContextVLA significantly improves π_0 , for example, ContextVLA achieves success rates of 69% in completing all 5 tasks consecutively, whereas π_0 achieves 60%. This demonstrates the effectiveness of ContextVLA on long-horizon tasks.

Table 8: **Results on CALVIN (ABC→D).** We report the success rates of consecutive completions (%) and average number of successes among 5 sequential subtasks (Avg. success length) of VLAs fine-tuned on the training dataset of CALVIN benchmark collected from environments A, B, and C.

Method	Success rates of consecutive completions (%)					Avg. success length
	1 / 5	2 / 5	3 / 5	4 / 5	5 / 5	
π_0 (Black et al., 2024)	90.95	82.53	74.00	66.95	59.58	3.740
+ ContextVLA (Ours)	93.38	92.70	85.80	77.58	69.36	4.238

918 E ADDITIONAL ANALYSIS
919

920 **Amortization Strategy.** We investigate the amortization strategy for obtaining a context token in
921 ContextVLA. To evaluate this, we fine-tune π_0 by
922 compressing past observations at a middle block
923 using three compression methods: global average
924 pooling, Perceiver Resampler (Alayrac et al., 2022;
925 Jain et al., 2024), and Attention Pooling (Ryoo et al.,
926 2024). In Table 9, we find that when compressing
927 past observations into a single token, average
928 pooling performs the best. For instance, on the
929 Simpler-WidowX benchmark, ContextVLA with aver-
930 age pooling achieves 56.2%, whereas using a Per-
931 ceiver Resampler yields only 53.0% when compress-
932 ing the observations into a single token. Notably,
933 Perceiver Resampler needs 64 tokens to show the
934 comparable performance of global average pooling,
935 highlighting the efficiency of our method in extract-
936 ing temporal context with extremely compressed to-
937 ken.

938 **The Number of Amortized Context Token.** We
939 investigate the appropriate number of context tokens
940 for utilizing the temporal context of historical obser-
941 vations to generate actions. To evaluate this,
942 we fine-tune π_0 with compressing past observations into $m = 1, 8$, or 64 tokens, by reshaping the
943 flattened tokens of length M into a tensor of shape $(m, M/m)$, and then applying average pooling
944 along the second dimension to obtain m tokens. In Table 9, we find that compressing historical
945 observations into a single token is the optimal choice, while compressing historical observations
946 into multiple context tokens still consistently outperforms the baseline π_0 that processes 8-frame
947 observations without compression.

948 **Visualization of Similarity of Amortized Context Token.** To analyze what information is pre-
949 served in the amortized context token, we calculate the cosine similarity of the context tokens and
950 visualize the normalized similarity matrix. Specifically, we calculate the similarity matrix of context
951 tokens obtained during conducting tasks from the Libero benchmark. In Figure 7, we find that sim-
952 ilar movement of the robot induces similar context tokens, indicating that context token preserves
953 the motion context of the robot rather than the static background or object.

954
955 F DETAILED ACTION GENERATION PROCESS
956

957 We here describe the detailed process of action generation of VLAs used in our framework: Au-
958 toregressive modeling (Kim et al., 2024; Pertsch et al., 2025), and diffusion-based modeling (Black
959 et al., 2024; Bjorck et al., 2025).

960
961 F.1 AUTOREGRESSIVE MODELING.

962
963 Autoregressive VLAs (O’Neill et al., 2024; Pertsch et al., 2025) encode a continuous robot action
964 $\mathbf{a}_{t:t+l}$ into discrete action tokens using an action tokenizer (Bu et al., 2025b; Pertsch et al., 2025),
965 and then train a Vision-Language Model (VLM) to generate the discrete action tokens via next
966 token prediction. Concretely, We first use the visual observations $\mathbf{o}_{t-k:t}$ and the text instruction \mathbf{c}_t
967 as a prompt for the VLM. And then, VLM autoregressively generates tokens, where we consider
968 the tokens as discretized action values. After the tokens are generated, we decode the tokens into
969 continuous action by using action de-tokenizer.

970 In our experiments, we use π_0 -FAST, which uses FAST tokenizer (Pertsch et al., 2025) for encod-
971 ing and decoding actions. The FAST tokenizer improves the compactness and expressivity of the
972 discretized action space by tokenizing actions in the frequency domain. Specifically, actions are

Table 9: Analysis of Amortization methods with different number of compressed tokens on Simpler-WidowX benchmark (Li et al., 2024b). All models are π_0 (Black et al., 2024) finetuned for 60K iterations with a batch size of 32, using the BridgeV2 dataset (Ebert et al., 2021). We report the averaged success rates (%) of the models on the benchmark.

Amortization	# tokens	Simpler-WidowX
Perceiver Resampler	1	53.0
	8	53.0
	64	56.0
Attention Pooling	1	52.0
	8	51.5
	64	53.0
Average Pooling	1	56.2
	8	56.0
	64	54.5
No compression	2048	47.8

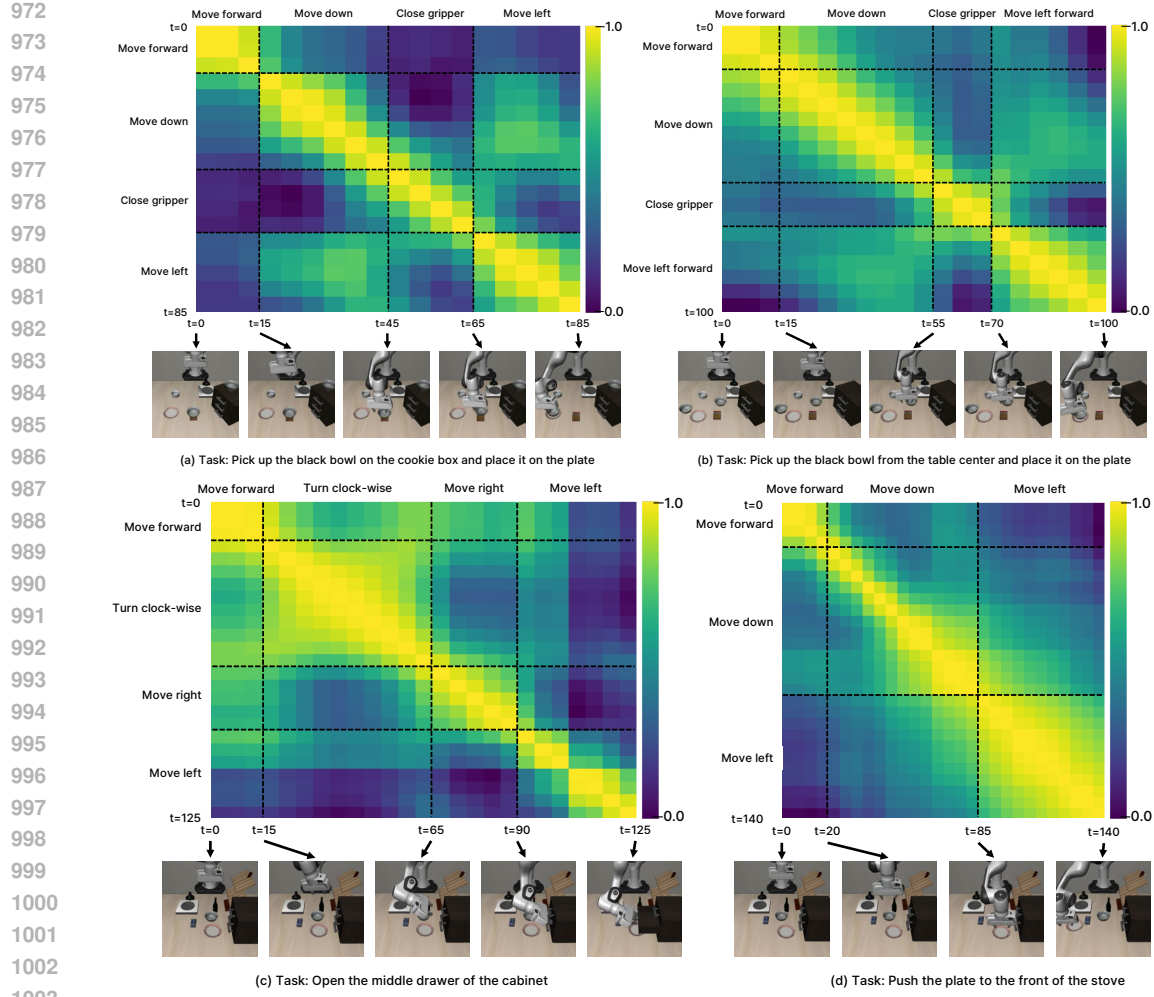


Figure 7: Visualization of the normalized cosine similarity matrix of context tokens obtained during conducting tasks from the Libero benchmark. We highlight the movement of the robot during the evaluation and the resulting visual observations on the matrix.

first transformed by a discrete cosine transform (DCT; Ahmed et al. 2006), then quantized and compressed into discrete tokens via byte-pair encoding (BPE; Gage 1994). These tokens are assigned to unused special tokens in the vocabulary of the VLM for training and generation.

F.2 DIFFUSION-BASED MODELING.

Diffusion-based VLAs (Black et al., 2024; Bjorck et al., 2025) generates action using diffusion model conditioned on a VLM. We first process the visual observation $\mathbf{o}_{t-k:t}$ and text instruction \mathbf{c}_t to extract high-level semantic information using VLM. Then, the extracted features are used as conditioning for Diffusion Transformer (DiT; Peebles & Xie 2022). Here, there are many approaches to condition the features on DiT, e.g., π_0 (Black et al., 2024) shares self-attention layers between VLM and DiT, and GR00T N1.5 (Bjorck et al., 2025) feeds the last hidden states of the VLM into cross-attention layer of DiT.

During Training, we sample denoising timestep $\tau \in [0, 1]$. Then, for the target action chunk $\mathbf{a}_{t:t+l}$ of the robot (Zhao et al., 2023; Chi et al., 2023), we add noise to the action using Gaussian noise $\epsilon \sim \mathcal{N}(\mathbf{0}, \mathbf{I})$:

$$\mathbf{a}_{t:t+l}^\tau = \tau \mathbf{a}_{t:t+l} + (1 - \tau) \epsilon. \quad (1)$$

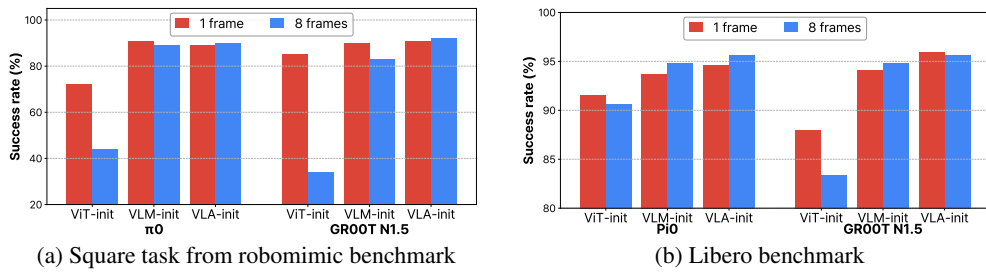
1026 Then, VLA model π_θ processes visual observation \mathbf{o}_t and text instruction \mathbf{c}_t to approximate the
 1027 denoising direction, *i.e.*, $\epsilon - \mathbf{a}_{t:t+l}$ by minimizing flow-matching loss:
 1028

$$1029 \mathcal{L} = \mathbb{E}_\tau \left[\left\| \pi_\theta(\mathbf{a}_{t:t+l}^\tau | \mathbf{o}_{t-k:t}, \mathbf{c}_t) - (\epsilon - \mathbf{a}_{t:t+l}) \right\|^2 \right]. \quad (2)$$

1032 During inference, we generate action $\mathbf{a}_{t:t+l}$ through denoising N steps. We sample random noise
 1033 $\mathbf{a}_{t:t+l}^0 \sim \mathcal{N}(\mathbf{0}, \mathbf{I})$, and apply ODE or SDE sampler to denoise it to generate action $\mathbf{a}_{t:t+l}$.
 1034

1036 G WEIGHT-INITIALIZATION ANALYSIS

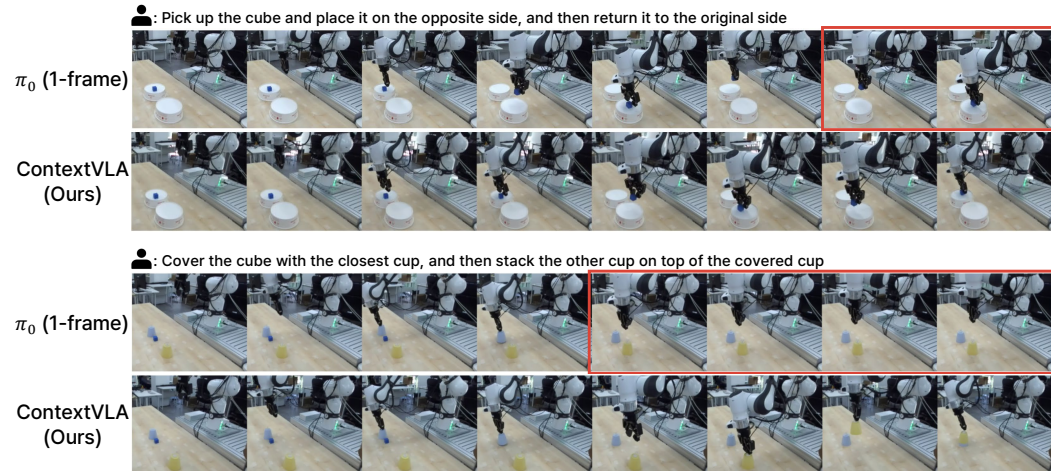
1038 In Figure 8, we analyze how different parameter initializations affect policy performance when using
 1039 multi-frame observation. We consider two architectures, π_0 (Black et al., 2024) and GROOT N1.5
 1040 (GEAR, 2025), and train them under three initialization schemes: (1) For ViT-init, only a vision
 1041 encoder is initialized with a pre-trained model (Zhai et al., 2023; Tschannen et al., 2025). (2) For
 1042 VLM-init, the vision encoder and VLM backbone are initialized with a pre-trained VLM (Beyer
 1043 et al., 2024; Chen et al., 2025). (3) For VLA-init, entire model is initialized with a pre-trained
 1044 VLA, *i.e.*, π_0 or GROOT N1.5. We observe that a policy model of VLA architecture but initialized
 1045 only with a vision encoder (*i.e.*, ViT-init) suffers from performance degradation when using multi-
 1046 frame inputs. In contrast, policies initialized with a pre-trained VLM or with VLA alleviate or even
 1047 overcome this issue, indicating the key factor in mitigating the problem is leveraging pre-trained
 1048 Vision-Language Model (VLM) to extract information for action generation.
 1049



1050 Figure 8: Success rates (%) of policy models of VLA architecture trained using either 1-frame or 8-
 1051 frame observations under different weight initialization schemes. ViT, VLM, and VLA-init indicate
 1052 how the VLA architecture is initialized for training; we use a pre-trained vision encoder, VLM, or
 1053 VLA, respectively, and other parameters are randomly initialized.
 1054

1065 H ADDITIONAL RELATED WORK

1068 **Multi-frame Observations for Behavior Cloning Policy** Many studies have observed that learning
 1069 behavior cloning (BC) policy with multi-frame observation can lead to performance degradation
 1070 (Muller et al., 2005; Bansal et al., 2019; Wang et al., 2019; Codevilla et al., 2019; De Haan et al.,
 1071 2019; Wen et al., 2020; Spencer et al., 2021; Seo et al., 2023; Torne et al., 2025). Early works have
 1072 shown that policies trained on multi-frame observations are prone to learn correlated features that
 1073 do not causally determine the expert actions (*i.e.*, spurious correlation; De Haan et al. 2019; Wen
 1074 et al. 2020; Spencer et al. 2021; Seo et al. 2023). This often produces the so-called copycat behav-
 1075 ior (Wen et al., 2020), where the policy ignores the observations and simply mimics the previous
 1076 actions as its next action. However, recently, Torne et al. (2025) has observed that diffusion policy
 1077 (Chi et al., 2023) shows a different trend to the traditional policies, where the model underutilizes
 1078 the past action, rather than mimicking the previous actions. In contrast, our work finds that recent
 1079 Vision-Language-Action (VLA) models show the opposite trend: they do not show the performance
 degradation commonly observed in traditional BC policies. Moreover, we introduce a method that
 effectively leverages multi-frame observations.

1080
1081
I QUALITATIVE RESULTS1082
1083 In Figure 9, we provide qualitative results for the real-world robotic tasks. We find that a policy that
1084 uses single-frame observations often fails to determine the correct next action, leading to failure in
1085 many cases, but ContextVLA leverages multi-frame observations to perform the task successfully.
10861102 **Figure 9: Qualitative results.** π_0 that uses single-frame observations fails to determine the correct
1103 next action due to the lack of utilizing temporal context (in red box), but ContextVLA leverages
1104 temporal context to determine the correct next action depending on the previous movement of a
1105 robot.
11061107
1108 **J ADDITIONAL QUANTITATIVE RESULTS**1109
1110 In Tables 10 and 11, we report performance of our method compared to the VLAs that uses 8-
1111 frame visual observations. We find that ContextVLA achieves performance comparable to, or even
1112 surpassing, the VLAs that use 8-frame observation without compression. This indicates that Con-
1113 textVLA effectively compresses past observations into an amortized token that captures the temporal
1114 context well.
11151116 **K USE OF AI TOOLS**1117
1118 We acknowledge that a large language model (LLM) was used to refine the phrasing and grammar
1119 of the manuscript.
1120
1121
1122
1123
1124
1125
1126
1127
1128
1129
1130
1131
1132
1133

1134 Table 10: **Results on Libero.** We report the success rates (%) of various VLAs fine-tuned on the
 1135 training dataset of Libero (Liu et al., 2023a).

Method	# frames	Spatial	Object	Goal	Long	Avg.
π_0 (Black et al., 2024)	1	96.3	97.3	96.2	88.8	94.7
π_0 (Black et al., 2024)	8	97.2	98.4	94.6	92.0	95.6
+ ContextVLA (Ours)	8	97.9	98.9	96.3	93.1	96.6
π_0 -FAST (Pertsch et al., 2025)	1	96.3	97.5	94.5	84.8	93.3
π_0 -FAST (Pertsch et al., 2025)	8	98.0	99.2	96.8	91.2	96.3
+ ContextVLA (Ours)	8	97.8	98.9	95.9	90.8	95.8
GR00T N1.5 (GEAR, 2025)	1	98.0	99.3	96.9	88.7	95.7
GR00T N1.5 (GEAR, 2025)	8	98.4	99.4	95.8	88.6	95.6
+ ContextVLA (Ours)	8	98.6	99.1	97.3	93.0	97.0

1147 Table 11: **Results on Simpler-WidowX.** We report the success rates (%) of various VLAs fine-tuned
 1148 on the Bridgev2 dataset (Walke et al., 2023).

Method	# frames	Spoon on Towel	Carrot on Plate	Stack Cube	Put Eggplant in Basket	Avg.
π_0 (Black et al., 2024)	1	46.5	38.7	42.7	39.3	41.8
π_0 (Black et al., 2024)	8	41.3	42.7	43.3	64.0	47.8
+ ContextVLA (Ours)	8	53.3	56.0	41.3	74.0	56.2
π_0 -FAST (Pertsch et al., 2025)	1	59.0	79.0	65.0	33.0	59.0
π_0 -FAST (Pertsch et al., 2025)	8	58.0	58.0	90.0	52.0	64.5
+ ContextVLA (Ours)	8	60.7	81.3	78.7	62.0	70.7
GR00T N1.5 (GEAR, 2025)	1	30.0	28.0	16.0	42.7	29.2
GR00T N1.5 (GEAR, 2025)	8	8.0	2.0	2.0	8.0	5.0
+ ContextVLA (Ours)	8	28.0	29.3	14.7	50.3	31.8

1161
 1162
 1163
 1164
 1165
 1166
 1167
 1168
 1169
 1170
 1171
 1172
 1173
 1174
 1175
 1176
 1177
 1178
 1179
 1180
 1181
 1182
 1183
 1184
 1185
 1186
 1187

1188

1189

1190

1191

1192

1193

1194

1195

1196

1197

1198

1199

1200

1201

1202

1203

1204

1205

1206

1207

1208

Table 12: **Full Results on Robocasa.** We report the success rates (%) of various VLAs fine-tuned on the training dataset of Robocasa (Nasiriany et al., 2024), consisting of 24 tasks with 100 demos per task

1211

1212

1213

1214

1215

1216

1217

1218

1219

1220

1221

1222

1223

1224

1225

1226

1227

1228

1229

1230

1231

1232

1233

1234

1235

1236

1237

1238

1239

1240

1241

Method	# frames	Pick and Place	Others	Avg.
π_0 (Black et al., 2024)	1	32.9	70.3	57.9
π_0 (Black et al., 2024)	8	35.8	70.8	59.1
+ContextVLA (Ours)	8	35.6	70.4	58.8
π_0 -FAST (Pertsch et al., 2025)	1	46.1	68.7	62.0
π_0 -FAST (Pertsch et al., 2025)	8	40.1	69.7	59.8
+ContextVLA (Ours)	8	48.6	68.7	62.0
GR00T N1.5 (GEAR, 2025)	1	51.8	67.6	62.3
GR00T N1.5 (GEAR, 2025)	8	53.0	67.0	62.3
+ ContextVLA (Ours)	8	52.8	70.2	64.4